

Wavelength-stable rare earth-free green light-emitting diodes for energy efficiency

Christian Wetzel^{1,2,*} and Theeradetch Detchprohm^{1,2}

¹Future Chips Constellation, Rensselaer Polytechnic Institute, Troy, New York 12180, USA

²Department of Physics, Applied Physics and Astronomy, Rensselaer Polytechnic Institute, Troy, New York 12180, USA

*wetzel@ieee.org

Abstract: Solid state lighting seeks to replace both, incandescent and fluorescent lighting by energy efficient light-emitting diodes (LEDs). Just like compact fluorescent tubes, current white LEDs employ costly rare earth-based phosphors, a drawback we propose to overcome with direct emitting LEDs of all colors. We show the benefits of homoepitaxial LEDs on bulk GaN substrate for wavelength-stable green spectrum LEDs. By use of non-polar growth orientation we avoid big color shifts with drive current and demonstrate polarized light emitters that prove ideal for pairing with liquid crystal display modulators in back light units of television monitors. We further offer a comparison of the prospects of non-polar *a*- and *m*-plane growth over conventional *c*-plane growth.

©2011 Optical Society of America

OCIS codes: (160.6000) Semiconductor materials; (250.5590) Quantum-well, -wire and -dot devices; (260.5430) Polarization.

References and links

1. I. Akasaki and C. Wetzel, "Future Challenges and Directions for Nitride Materials and Light Emitters," Proc. IEEE **85**(11), 1750–1751 (1997), <http://dx.doi.org/doi:10.1109/5.649652>.
2. O. Jani, I. Ferguson, C. Honsberg, and S. Kurtz, "Design and characterization of GaN/InGaN solar cells," Appl. Phys. Lett. **91**(13), 132117 (2007), <http://dx.doi.org/doi:10.1063/1.2793180>.
3. P. Schlotter, R. Schmidt, and J. Schneider, "Luminescence conversion of blue light emitting diodes," Appl. Phys., A Mater. Sci. Process. **64**(4), 417–418 (1997), <http://dx.doi.org/doi:10.1007/s003390050498>.
4. C. Wetzel, T. Salagaj, T. Detchprohm, P. Li, and J. S. Nelson, "GaInN/GaN Growth Optimization for High Power Green Light Emitting Diodes," Appl. Phys. Lett. **85**(6), 866 (2004), <http://dx.doi.org/doi:10.1063/1.1779960>.
5. G. Chen, M. Craven, A. Kim, A. Munkholm, S. Watanabe, M. Camras, W. Götz, and F. Steranka, "Performance of high-power III-nitride light emitting diodes," Phys. Status Solidi **205**(5), 1086–1092 (2008), <http://dx.doi.org/doi:10.1002/pssa.200778747> (a).
6. H. Amano, N. Sawaki, I. Akasaki, and Y. Toyoda, "Metalorganic vapor phase epitaxial growth of a high quality GaN film using an AlN buffer layer," Appl. Phys. Lett. **48**(5), 353 (1986), <http://dx.doi.org/doi:10.1063/1.96549>.
7. D. Hanser, M. Tutor, E. Preble, M. Williams, X. P. Xu, D. Tsvetkov, and L. H. Liu, "Surface preparation of substrates from bulk GaN crystals," J. Cryst. Growth **305**(2), 372–376 (2007), <http://dx.doi.org/doi:10.1016/j.jcrysgro.2007.03.039>.
8. T. Takeuchi, C. Wetzel, S. Yamaguchi, H. Sakai, H. Amano, I. Akasaki, Y. Kaneko, S. Nakagawa, Y. Yamaoka, and N. Yamada, "Determination of Piezoelectric Fields in GaInN Strained Quantum Wells Using the Quantum-Confined Stark Effect," Appl. Phys. Lett. **73**(12), 1691–1693 (1998), <http://dx.doi.org/doi:10.1063/1.122247>.
9. C. Wetzel, T. Takeuchi, H. Amano, and I. Akasaki, "Piezoelectric Franz-Keldysh Effect in Strained GaInN/GaN Heterostructures," J. Appl. Phys. **85**(7), 3786–3791 (1999), <http://dx.doi.org/doi:10.1063/1.369749>.
10. C. Wetzel, Rump Session; The Second International Conference on Nitride Semiconductors - ICNS 97, 27–31 October 1997, Tokushima, Japan.
11. R.F. Karlicek, Jr., "UV-LEDs and Curing Applications," Radtech Report, Nov/Dec 2009, pp. 17–23.
12. W. Zhao, Y. Li, Y. Xia, M. Zhu, T. Detchprohm, E. F. Schubert, and C. Wetzel, "Analysis of Quantum Efficiency of GaInN/GaN Light Emitting Diodes in the Range of 390 - 580 nm," in "GaN, AlN, InN, and Related Materials," Eds. M. Kuball, T.H. Myers, J.M. Redwing, T. Mukai, Proc. Mat. Res. Soc. Symp. Vol. **892**, FF12.2 (2006).
13. S. You, T. Detchprohm, M. Zhu, W. Hou, E. A. Preble, D. Hanser, T. Paskova, and C. Wetzel, "Highly polarized green light emitting diode in m-axis GaInN/GaN," Appl. Phys. Exp. **3**, 102103 (2010), <http://dx.doi.org/doi:10.1143/APEX.3.102103>

14. T. Detchprohm, M. Zhu, Y. Li, Y. Xia, L. Liu, D. Hanser, and C. Wetzel, "Growth and Characterization of Green GaInN-Based Light Emitting Diodes on Free-Standing Non-Polar GaN Templates," *J. Cryst. Growth* **311**(10), 2937–2941 (2009), <http://dx.doi.org/doi:10.1016/j.jcrysgro.2009.01.060>.
15. T. Detchprohm, M. Zhu, W. Zhao, Y. Wang, Y. Li, Y. Xia, and C. Wetzel, Enhanced Device Performance of GaInN-Based Deep Green Light Emitting Diodes with V-Defect-Free Active Region," *Phys. Stat. Solidi C* **6**(S2), S840–S843 (2009), <http://dx.doi.org/doi:10.1002/pssc.200880800>
16. M. Zhu, Y. Xia, W. Zhao, Y. Li, J. Senawiratne, T. Detchprohm, and C. Wetzel, "Structural Characterization of Homoepitaxial Blue GaInN/GaN Light-Emitting Diodes by Transmission Electron Microscopy," *J. Electron. Mater.* **37**(5), 641–645 (2008), <http://dx.doi.org/doi:10.1007/s11664-008-0392-9>.
17. T. Detchprohm, M. Zhu, Y. Li, Y. Xia, C. Wetzel, E. A. Preble, L. Liu, T. Paskova, and D. Hanser, "Green Light Emitting Diodes on a-Plane GaN Bulk Substrates," *Appl. Phys. Lett.* **92**(24), 24119 (2008), <http://dx.doi.org/doi:10.1063/1.2945664>.
18. T. Detchprohm, M. Zhu, Y. Li, L. Zhao, S. You, C. Wetzel, E. A. Preble, L. Liu, T. Paskova, and D. Hanser, "Wavelength-Stable Cyan and Green Light Emitting Diodes on Non-Polar m-Plane GaN Bulk Substrates," *Appl. Phys. Lett.* **96**(5), 051101 (2010), <http://dx.doi.org/doi:10.1063/1.3299257>.
19. M. Zhu, S. You, T. Detchprohm, T. Paskova, E. A. Preble, D. Hanser, and C. Wetzel, "Inclined Dislocation Pair Relaxation Mechanism in Homoepitaxial Green GaInN/GaN Light Emitting Diodes," *Phys. Rev. B* **81**(12), 125325 (2010), <http://dx.doi.org/doi:10.1103/PhysRevB.81.125325>.
20. C. Wetzel, M. Zhu, Y. Li, W. Hou, L. Zhao, W. Zhao, S. You, C. Stark, Y. Xia, M. DiBiccari, and T. Detchprohm, "Green LED development in polar and non-polar growth orientation," Ninth International Conference on Solid State Lighting, Proc. SPIE Vol. **7422**, 742204 (Aug. 18, 2009). <http://dx.doi.org/doi:10.1117/12.829513>
21. K. Kojima, H. Kamon, M. Funato, and Y. Kawakami, "Theoretical investigations on anisotropic optical properties in semipolar and nonpolar InGaN quantum wells," *Phys. Stat. Solidi C*, **5**, 3038 (2008). <http://dx.doi.org/doi:10.1002/pssc.200779277>
22. H. Masui, H. Yamada, K. Iso, S. Nakamura, S. P. DenBaars, "Optical polarization characteristics of m-oriented InGaN/GaN light-emitting diodes with various indium compositions in single-quantum-well structure," *J. Phys. D Appl. Phys.* **41**(22), 225104 (2008), <http://dx.doi.org/doi:10.1088/0022-3727/41/22/225104>.
23. M. Kubota, K. Okamoto, T. Tanaka, and H. Ohta, "Temperature dependence of polarized photoluminescence from nonpolar m-plane InGaN multiple quantum wells for blue laser diodes," *Appl. Phys. Lett.* **92**(1), 011920 (2008), <http://dx.doi.org/doi:10.1063/1.2824886>.
24. N. Fellows, H. Sato, H. Masui, S. P. DenBaars, and S. Nakamura, "Increased Polarization Ratio on Semipolar (11-22) InGaN/GaN Light-Emitting Diodes with Increasing Indium Composition," *Jpn. J. Appl. Phys.* **47**(10), 7854–7856 (2008), <http://dx.doi.org/doi:10.1143/JJAP.47.7854>.
25. C. H. Chiu, S. Y. Kuo, M. H. Lo, C. C. Ke, T. C. Wang, Y. T. Lee, H. C. Kuo, T. C. Lu, and S. C. Wang, "Optical properties of a-plane InGaN/GaN multiple quantum wells on r-plane sapphire substrates with different indium compositions," *J. Appl. Phys.* **105**(6), 063105 (2009), <http://dx.doi.org/doi:10.1063/1.3083074>.
26. S. E. Brinkley, Y.-D. Lin, A. Chakraborty, N. Pfaff, D. Cohen, J. S. Speck, S. Nakamura, and S. P. DenBaars, "Polarized spontaneous emission from blue-green m-plane GaN-based light emitting diodes," *Appl. Phys. Lett.* **98**, 011110 (2011), <http://dx.doi.org/doi:10.1063/1.3541655>
27. M. Zhu, S. You, T. Detchprohm, T. Paskova, E. A. Preble, and C. Wetzel, "Various Misfit Dislocations in Green and Yellow GaInN GaN Light Emitting Diodes," *Phys. Status Solidi., A Appl. Mater. Sci.* **207**(6), 1305–1308 (2010), <http://dx.doi.org/doi:10.1002/pssa.200983645>.
28. C. Wetzel, Y. Li, J. Senawiratne, M. Zhu, Y. Xia, S. Tomasulo, P. D. Persans, L. Liu, D. Hanser, and T. Detchprohm, "Characterization of GaInN/GaN layers for green emitting laser diodes," *J. Cryst. Growth* **311**(10), 2942–2947 (2009), <http://dx.doi.org/doi:10.1016/j.jcrysgro.2009.01.067>.
29. W. Zhao, Y. Li, Y. Xia, M. Zhu, T. Detchprohm, E. F. Schubert, and C. Wetzel, "Analysis of Quantum Efficiency of GaInN/GaN Light Emitting Diodes in the Range of 390 - 580 nm," in "GaN, AlN, InN, and Related Materials," Eds. M. Kuball, T.H. Myers, J.M. Redwing, T. Mukai, Proc. Mat. Res. Soc. Symp. Vol. **892**, FF12.2 (2006).

1. Solid-state lighting for energy efficiency

Few things have changed as little as the way we light our living rooms. Yet almost synonymous with ingenuity, the incandescent light bulb is set to take the path of gas guzzler cars. In light of rising atmospheric carbon levels, energy takes on the status of a new lead currency. Solid-state lighting has taken on the goal to replace wastefully inefficient incandescent lighting and is on its way to outrun fluorescent lamps as well. Light emitting diodes (LEDs) and their organic cousins OLEDs are the prime contenders for high intensity and large area light sources, respectively. Key to both is the availability of a pn-junction in direct wide bandgap semiconductors. Indeed, the alloys of AlGaInN group-III nitrides allow for coverage of the entire visible spectrum of light and besides efficient LEDs [1], should also prove ideal for multijunction solar cells [2]. The present best LEDs indeed employ a blue emitting GaInN/GaN quantum well structure within a GaN pn-junction. To render a full white spectrum, they convert a good portion of light to the longer wavelengths by help of a

phosphor [3]. Yet this is a point where significant new losses come into play. Moreover, such phosphors heavily rely on increasingly expensive rare earth elements of terbium, erbium, yttrium, and europium. Our approach therefore is to supply all those longer wavelength colors also by direct emitting GaInN/GaN quantum wells, which requires a rather high alloy fraction of InN [4]. The amount of indium required in this approach is still far less than the need of rare earth elements in the phosphor approach. The major challenges, however, are those of a performance droop with high injection densities and with longer emission wavelength (“green gap” problem) [5].

2. The case for bulk GaN substrate

How to prepare a layered electronic device structure from a material that wants to grow as a thin whisker only? *c*-plane sapphire offers lattice structure and constants close to wurtzite GaN and thanks to low temperature deposited buffer layers [6], the remaining difference can be overcome, yet at the cost of very high densities of threading dislocations aligned with the growth direction. How could the intrinsic properties of a material be identified and the ultimate performance of LEDs be foreseen if every modeling parameter needs to be indexed by the dislocation density? The answer must lie in the development of dislocation-free bulk GaN of reasonable size to accommodate a range of experimental devices suitable to explore just what could be possible in the absence of dislocations [7].

The anisotropy of preferred whisker growth and threading dislocations stems from the uniaxial nature of the wurtzite crystal structure of GaN. The same gives rise to inversion asymmetry along the unique *c*-axis and is commensurate with the presence of large piezoelectric fields of MV/cm. From our observation of a quantum confined Stark effect [8] and direct quantification of huge electric fields from pronounced Franz-Keldysh oscillations [9], we concluded, that the optoelectronic properties of group-III nitride heterostructures should primarily be controlled by those electric fields [10].

Despite a very wide variety of approaches, GaInN/GaN heterostructure light emitting devices show an almost uniform efficiency maximum near 450 nm with steep drops to shorter as well as to longer wavelength ranges (“green gap” problem) [11]. Moreover, high performance light emitters show a nearly universal maximum of light generation efficiency in a narrow injection current density range of 1 – 10 A/cm² (the so called issue of “droop”) [12].

Given the prevalent role of piezoelectric polarization in such structures, it is reasonable to hypothesize that both issues could also be a direct consequence of the uniaxial crystal structure and its piezoelectric polarization.

The recent availability of low-dislocation density bulk GaN crystals of the volume of cm³ therefore provides the opportunity to avoid the detriment of threading dislocations while at the same time allowing attenuation and even inversion of piezoelectric polarization by homoepitaxial growth of heterostructures along a large variety of higher index crystal axes between *c*-axis and *c*-plane. Quantum confinement along such directions further breaks the symmetry of the valence band in Γ to lift degeneracy of the two topmost hole states.

In the case of nonpolar growth of GaInN/GaN quantum wells along the *a*- and *m*-axes of GaN we so find two highly desirable aspects for full spectrum direct emitting LEDs: in absence of piezoelectric polarization along the quantum well (QW) axis, emission wavelength remains unaffected by the injection drive current density and the top surface emission of the LED is linearly polarized to a very high degree. The first aspect allows for color stable light sources throughout the blue, green, and potentially even yellow and red spectral regions. The second can avoid generation of light that would be lost whenever combined with polarization sensitive modulators such as in liquid crystal display technology as used in television monitors.

3. Experimental

In our approach low dislocation density bulk GaN substrate was obtained by rapid growth along the *c*-axis in hydride vapor phase epitaxy on sapphire substrate leading to 50 mm diameter boules of up to 7 mm thickness. By means of a seeded annihilation process,

threading dislocation densities can be reduced to values as low as $5 \times 10^6 \text{ cm}^{-2}$. Cuts along polar c -plane ($10 \times 10 \text{ mm}^2$) and non-polar a - and m -planes ($5 \times 10 \text{ mm}^2$) have been polished chemo-mechanically for epitaxy-ready surface preparation. All of the above were commercially prepared by and obtained from Kyma Technologies, Inc [7].

GaNIn/GaN quantum well structures were grown homoepitaxially by metal organic vapor phase epitaxy in vertical flow geometry. On top of a $1 \mu\text{m}$ -thick Si-doped n-GaN layer followed a nominally undoped active region of 8 or 10 pairs of $3 \text{ nm Ga}_{1-x}\text{In}_x\text{N}$ QWs embedded in $20 - 25 \text{ nm GaN}$ barriers [13]. InN-fractions x and well widths were determined by combining the multi QW-averaged alloy composition from x-ray diffraction with the actual layer thicknesses as derived from high resolution transmission electron microscopy (TEM) [14]. Full LED structures in addition were capped off by a $15 \text{ nm Al}_{0.18}\text{Ga}_{0.82}\text{N}$ electron blocking layer and $80 \text{ nm } p\text{-GaN}$ [13]. For photoluminescence (PL), a 325 nm line of a HeCd laser at a beam power density of 10 mW/mm^2 was used. The top surface emission in electroluminescence (EL) and PL was analyzed by a linear polarizer and detected by a photospectrometer. For temperature dependent PL, a 408 nm laser diode was used for excitation. Unless noted otherwise, LED dies were fabricated with a top contact mesa structure geometry in photolithography and inductively coupled remote plasma etching.

4. Results

Approaches to avoid the formation of structural defects proved crucial to controllably extend the emission wavelength from the 450 nm blue over 525 nm green into 560 nm yellow and 580 nm orange spectral regions. Ample evidence in the literature points to the formation of sizable V-defects originating in the intersection of threading dislocations with GaInN quantum wells. We find that growth of subsequent layers is strongly affected by such defects leading to the formation of highly irregular quantum wells and the loss of light emission efficiency. By tight control of the quantum well growth conditions, we have been able to virtually eliminate the formation of such V-defect generation in quantum well structures at least up to 580 nm of emission wavelength [15].

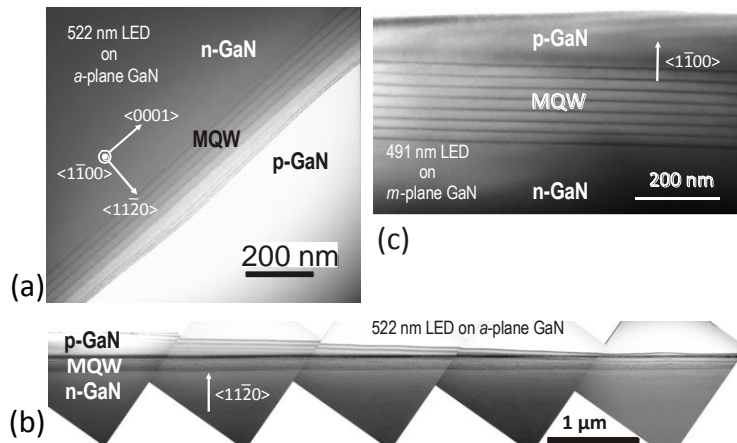


Fig. 1. Cross sectional transmission electron micrographs of the active region in homoepitaxially grown GaIn/GaN LED structures revealing absence of structural defects and highly uniform quantum well regions. a) green a -plane structure; b) the same viewed over a length of $7.4 \mu\text{m}$; c) a cyan m -plane structure. After [17,18]

Homoepitaxy on such prepared low dislocation density bulk GaN can be performed without any loss of crystalline perfection. In fact, an interface between template and epitaxially overgrown layers cannot be identified by various tested methods including high resolution cross sectional TEM [16]. By epitaxial growth on the m - and a -plane side planes of c -axis grown bulk templates, the remaining c -axis oriented threading dislocations are furthermore effectively buried and cannot propagate along the newly defined growth

directions. Up to an emission wavelength of around 500 nm we so achieve virtual threading dislocation free GaN and GaInN/GaN quantum well growth in all of c -axis, m -axis, and a -axis growth (Fig. 1) [16–18]. Comparing the achieved performance of a -plane and m -plane material we find a propensity to generate misfit dislocations on the a -plane that become apparent as line defects on the growth surface and are likely to lead to inhomogeneous layer thicknesses of the active quantum well region. On m -plane material, however, we do not find any indications of such problems.

The absence of threading dislocations furthermore allows for the growth of highly uniform quantum wells as verified on cross sectional TEM over lateral stretches of several micro meter [17]. The perfect template, however, is found to give rise to a new high density defect in the case of high InN-fraction GaInN alloy quantum wells as utilized for emission wavelengths beyond 500 nm. With a very high regularity, in polar c -plane growth, we observe the formation of inclined dislocation pairs within the first few quantum wells without the apparent presence of any precursor defects [19]. Pairs are seen to originate within the same atomic layer within a lateral separation of some 20 nm and then separate with progressing layer growth with an inclination of about 20 degrees from the c -axis. In planar view, the pair branches are found to separate with either 180 or 120 degrees of separation [19]. We have ascribed this inclination to a dislocation climb by means of the Peach-Koehler force. With progressing growth, the dislocations separate further increasing the area of lower biaxial strain behind. We consider this relaxation mechanism as the driving force for the dislocation climb. The observed dislocation density reaches the very high value of $5 \times 10^9 \text{ cm}^{-2}$ and the observed LED performance limitations most likely are a consequence thereof [19].

It can be speculated that the large lattice mismatch between the initiating GaInN layer on the virtually defect-free GaN barriers first induces stacking faults that then lead to the formation of the observed inclined dislocation pairs. A direct observation so far, however, has not been possible.

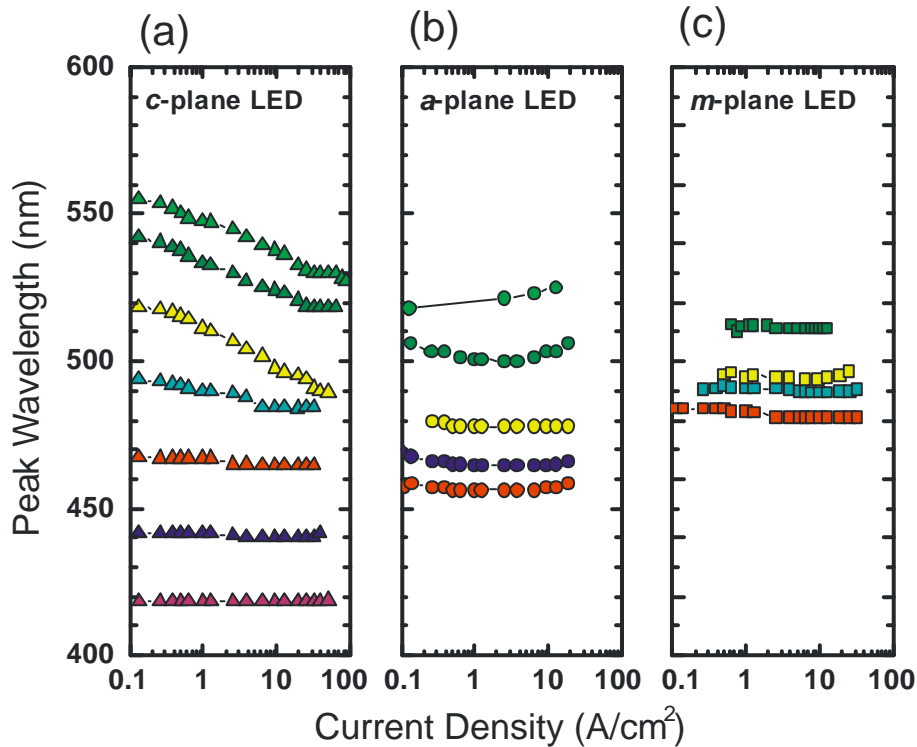


Fig. 2. Peak wavelength versus current density in (a) polar *c*-plane, (b) non-polar *a*-plane, and (c) non-polar *m*-plane LEDs. In the polar structures, wavelength stability is satisfactory only for blue LEDs, while non-polar structures offer the same also in the green. After [17,18].

We find that LED emission wavelength strongly varies between polar *c*-plane and non-polar *m*- and *a*-plane structures even if similar quantum well growth conditions are offered [20]. Under the reasonable assumption of an unclamped lattice expansion along the growth axis, asymmetric biaxial strain conditions of the quantum wells can be interpolated also for growth along the non-polar orientations. From this, the actual InN alloy fractions can be determined by ω -2 θ x-ray diffraction analysis utilizing actual layer thicknesses as determined in high resolution TEM. We find that in contrast to the polar *c*-plane material, roughly twice as high InN fractions in wells of similar thickness are required in the non-polar orientations to reach the same green and deep green spectral regions. We attribute this to the wavelength extending aspects of the piezoelectric polarization dipole in the *c*-plane structures, typically ascribed to the quantum confined Stark effect [8]. This electrostatic effect, however, is strongly affected by dynamical screening as carrier densities are varied with variations of the LED drive current density.

In the consequence, polar *c*-plane LED structures show a significant blue shift with increasing drive current. What may start out as a green LED at 1 A/cm² likely turns into a cyan or even blue LED at 35 A/cm². Such color variation is detrimental for most LED lighting applications. Therefore, an avoidance of the polarization dipole normal to the quantization plane is highly desirable. This can effectively be achieved in non-polar structures such as in *a*- and *m*-plane oriented LEDs. For a comparison of peak wavelength versus LED current density in scratch diode geometry, see Fig. 2. Apparently, in non-polar structures we find peak wavelength variations in the green of not more than a few nanometers.

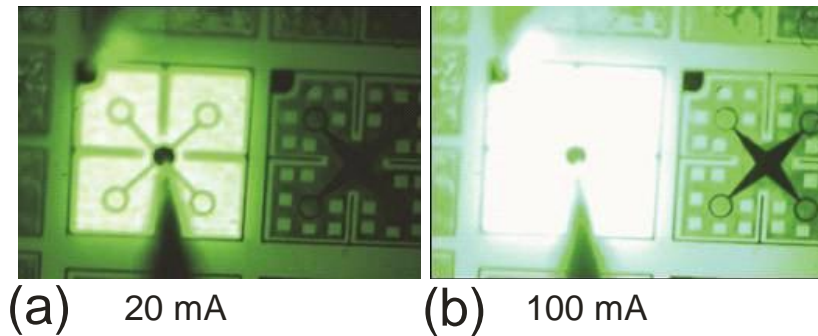


Fig. 3. Non-polar 520 nm green LED die ($700 \times 700 \mu\text{m}^2$) on m -plane bulk GaN substrate. There is only a minimal change of color as the current is varied from 20 mA to 100 mA.

A typical m -plane green LED in operation under low (20 mA) and high (100 mA) current is shown in Fig. 3. Figure 4 maps the color loci on the 1931 CIE color coordinate diagram (color schematic only) as a function of drive current. Large color variation is seen in the polar structures (Fig. 4a) while color variation remains minimal in the non-polar case (Fig. 4b). With such high color stability, non-polar structures are particularly suited for direct emitting all-color LEDs bypassing the inefficient step of photon down conversion in costly rare earth element phosphors (see Fig. 3).

Such non- c -plane oriented quantum wells have additional benefits for the efficient light generation. The asymmetric biaxial strain condition in the layer plane will lift the energetic degeneracy of the two top-most spin-orbit coupled valence bands. Both, in non-polar m -plane and a -plane growth this leads to a higher transition energy for electric dipole radiation oriented along the c -axis. Consequently, carrier recombination through the other, higher lying valence band is strongly favored leading to an effective reduction of the density of states for holes. Such a condition has been demonstrated in other systems to lead to a lower excitation threshold for carrier distribution inversion and a resulting lower threshold for stimulated emission.

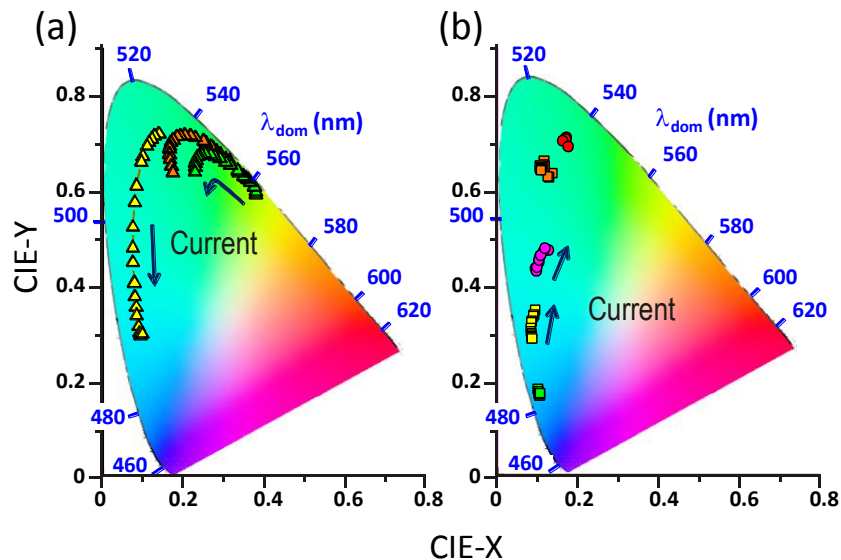


Fig. 4. CIE 1931 color loci of a) c -plane polar and b) a - and m -plane non-polar LEDs as current is varied in the range of $0.1 - 100 \text{ A/cm}^2$. Perceived cyan and green colors remain stable only in the non-polar LED structures. Symbols correspond to those in Fig. 2.

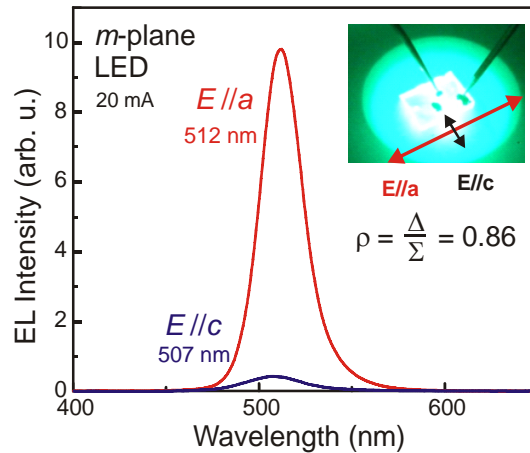


Fig. 5. Linear polarization analyzed emission spectra of the top emission of a green *m*-plane LED. Spectra differ in peak wavelength and intensity revealing a polarization ratio $\rho = 0.85$. Inset: the LED in operation which schematics of the polarization geometry.

The lifting of the degeneracy furthermore leads to the generation of light with only a single orientation of the electric dipole radiation, i.e., linear polarized light emission from the planar surfaces of the LED (Fig. 5) [21]. In contrast to a passive polarizer operating on the principle of selective absorption, this active polarized light emitter does not waste electrical excitation on the unwanted portion of light. Experimental polarization ratios, defined by the maximum intensity difference of orthogonal polarizations as a fraction of total intensity, is shown in Fig. 6. Data derived in this work from photoluminescence and electroluminescence is compared to data of the literature [22–26]. For the green spectral region, *m*-plane structures offer the highest degree of polarization. The ratio proves to increase with wavelength.

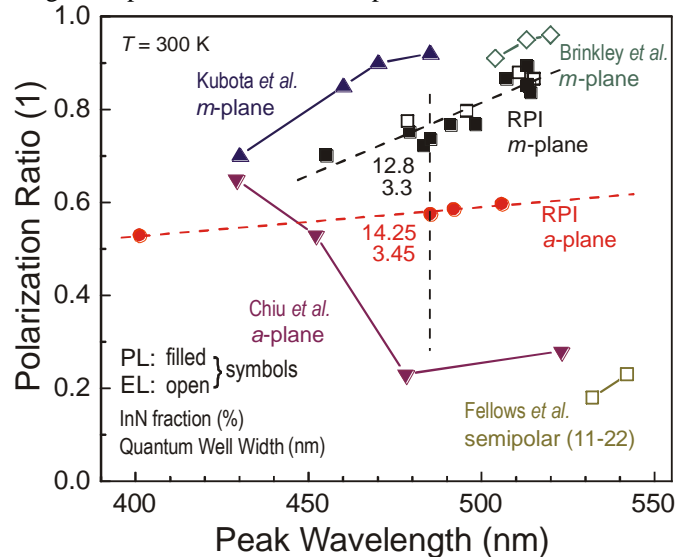


Fig. 6. Emission polarization ratio versus peak wavelength in PL and EL of this and other work for various growth orientations. *m*-plane structures offer the highest values and a trend to increase with wavelength. After [13].

LEDs of linear polarized light emission are particularly suited for pairing with liquid crystal modulators which can only transmit one single polarization of light. By help of polarization preserving optics, e.g., metallic mirrors, such LEDs could serve in energy efficient back light units for liquid crystal displays (LCDs) as used in general purpose

monitors. By avoiding the big filter losses in passive polarizers, such polarized LED-LCD combinations should exhibit a substantial gain to the system energy efficiency.

A comparison of achieved light output power in LEDs of the different growth directions naturally will reflect a current best effort result. Measured at the wafer level in scratch diode geometry at a current density of 12.6 A/cm^2 and light detected through the substrate side only, the following partial light output powers have recently been achieved in our efforts. In polar growth on *c*-plane sapphire, 6 – 7 mW at 450 nm, 2 – 5 mW at 540 nm. For green LEDs on *c*-plane bulk GaN, the same values have been achieved [27]. In non-polar *a*-plane growth on bulk GaN, 500 – 600 μW at 480 nm and 160 μW at 520 nm have been achieved [17]. In non-polar *m*-plane growth on bulk GaN, 2 mW at 490 nm, 400 μW at 510 nm, 30 μW at 520 nm, and 10 μW at 540 nm have been achieved [18].

These results may suggest a general superiority of the polar *c*-plane growth on sapphire over all other approaches including *c*-plane growth on bulk GaN. Care, however must be taken to make a fair comparison within those wafer level measurements. For once, the wide and inexpensive availability of sapphire substrates reflects in a far higher developed fine tuning of growth recipes in our reactors over the generally very limited wafer size and wafer count of bulk GaN material. On the other hand, light extraction through the back of a thin GaN structure on sapphire is inherently higher than on a thick planar GaN slab. For the non-polar growth, it must be noted that by continued effort the mW power range has been reached in the long wavelength blue using *m*-plane bulk GaN, while a more limited effort on *a*-plane material trails this comparison.

An estimate of the internal quantum efficiency (IQE) frequently is given by comparing PL efficiencies at different sample temperatures. Using direct photoexcitation of the QW over a wide range of excitation powers, both, at room temperature and at 4 K, an upper limit of IQE at room temperature is shown in Fig. 7. Included are polar *c*-plane structures on sapphire and non-polar *a*- and *m*-plane structures on bulk GaN. Assuming a total absorption in the QWs of 16% of the incident beam power, the discussed current density of 12 A/cm^2 roughly corresponds to a laser power intensity of 240 W/cm^2 (indicated by a dashed line).

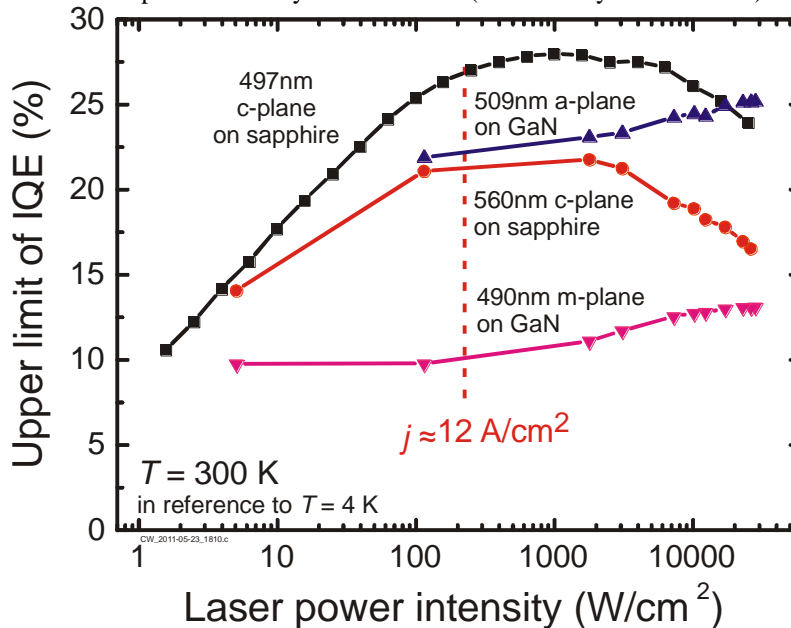


Fig. 7. Upper limit of the internal quantum efficiency as a function of incident 408 nm optical beam power density. Room temperature data was obtained by scaling to the respective PL maximum at $T = 4 \text{ K}$. Most interestingly, under highest excitation, values in *a*-plane material surpass those of *c*-plane material at similar wavelength.

From this data it can be seen that similar to droop in electrical measurements, IQE drops with higher excitation density in the polar *c*-plane material [28]. In contrast, both, the non-polar *a*- and *m*-plane structures show an increase of efficiency with increasing optical excitation density. Such a behavior has previously been seen in low performing *c*-plane material [29], and may not necessarily be proof of higher overall performance. Yet, for the case of *a*-plane material under highest excitation, IQE even surpasses that of *c*-plane on sapphire material of even shorter emission wavelength. Although derived from an as yet limited set of samples, such a behavior is of particular promise for the identification of the best possible growth geometry.

Therefore, while the overall measured light output performance of non-polar *a*-plane material is trailing our comparison, the higher crystalline quality of the active region as observed by the absence of threading dislocations in TEM of Fig. 1 lends particular credibility to the superior trend of high and improving internal quantum efficiency with high efficiency at wavelengths as long as 509 nm and beyond.

7. Conclusion

In summary we demonstrated color-stable phosphor-free direct-emitting green LEDs. We find that homoepitaxy on bulk GaN substrate can achieve active layers in all of, polar *c*-plane, non-polar *a*-plane and non-polar *m*-plane growth. In the non-polar structures, we effectively suppress any color variation known to occur in regular *c*-plane structures under a variation of drive current. Those non-polar structures also allow the realization of highly linear polarized LEDs which allows a reduction in power losses when combined with liquid crystal polarizers such as used in television monitors. At present, we achieve active region growth devoid of any structural defects up to emission wavelengths of some 500 nm in all those growth orientations. Yet for *a*-plane material, such crystalline perfection has been achieved to wavelength as long as 509 nm.

While highest overall light output power has been achieved in conventional *c*-plane growth, the trend of increasing internal quantum efficiency with higher excitation density in the non-polar structures, is a highly promising aspect of such growth orientations. As judged from PL-based values for this efficiency, 509 nm green *a*-plane material is found to increase even beyond the values of 497 nm *c*-plane based material. This quintessential anti-droop behavior at high efficiency can be interpreted as a particular promising sign for such structures for further increased efficiencies at even longer wavelength regions of the green including the yellow and red.

Acknowledgments

We would like to acknowledge E.A. Preble, T. Paskova, and D. Hanser (currently with SRI International, Inc.) at Kyma Technologies, Inc. for providing bulk GaN substrates of different crystal orientations. The authors are in debt to Yong Xia, Mingwei Zhu, Wei Zhao, Shi You, Wenting Hou, Liang Zhao, and Christoph Stark for their active role in the compilation of this data. This work was supported by a United States of America Department of Energy National Energy Technology Laboratory (DOE/NETL) Solid-State Lighting Contract of Directed Research under DE-FC26-06NT42860. This work was also supported by the National Science Foundation (NSF) Smart Lighting Engineering Research Center (# EEC-0812056) and by the New York State Foundation for Science, Technology, and Innovation (NYSTAR) under contract C090145.